Enhancement of H^- Volume Production in Double Plasma Discharge

Osamu Fukumasa and Hideki Nishimura

Department of Electrical and Electronic Engineering,
Faculty of Engineering, Yamaguchi University, Ube 755, Japan

(Received)

The production of hydrogen negative ions H^- in a pure volume source has been studied. In our double plasma negative ion source, both energy and density of fast electrons are well controlled. Using this source, enhancement of H^- production has been achieved. The extracted H^- current in the double plasma operation is higher than that in the single plasma operation when observed under the same discharge power. Measurements of plasma parameters in the source and in the extractor regions have been carried out for both cases. Enhancement of H^- production is achieved by optimizing plasma parameters for a so-called two-step process of H^- volume production.

KEYWORDS: negative ion source, volume production, vibrationally excited molecules, magnetic filter, double plasma discharge

According to our numerical simulation results,[1,2] most H^- ions are produced by a two-step process.[3] Namely, H^- ions are generated by dissociative attachment of slow plasma electrons e (with electron temperature $\kappa T_e \sim 1$ eV) to highly vibrationally excited molecules $H_2(v'')$ (effective vibrational level $v'' \geq$ 5-6), and these $H_2(v'')$ are mainly produced by collisional excitation of fast electrons e_f with energies in excess of 20-30 eV. Recently, to test the H^- volume production process, we have developed a double plasma (DP) negative ion source,[4] where plasma parameters, especially the energy and density of e_f, are well controlled by manipulating the injected beam parameters, i.e., beam acceleration voltage V_B and beam current I_B. Using this source, the effect of e_f on H^- production is investigated,[5] and the results qualitatively support the two-step H^- production process.

In this work, with the use of this DP negative ion source, we will study mainly H^- production (i.e., enhancement of H^- production due to optimization of e_f distribution caused by double plasma operation) and discuss briefly its isotope effect (i.e., H^-/D^- production). The comparison of data for hydrogen H_2 and deuterium D_2 is important in order to understand the reasons underlying the differences in performances for volume D^- sources and H^- sources.

Figure 1 shows a schematic diagram of the DP negative ion source.[4,5] The source chamber is made of stainless steel, and is divided by a mesh grid into two regions, a driver plasma region (the left-hand side) and a target plasma region (the right-hand side). The target plasma region is a conventional multicusp volume source of negative ions equipped with both a magnetic filter and a plasma grid. The plasma conditions are determined by the discharge current I_d and the discharge voltage V_d for the driver plasma, the acceleration voltage V_B (i.e., the potential difference between two chambers) and the gas pressure p. In the present experiment, V_d is fixed at 40 V. Electrons in the driver plasma are extracted and injected into the target chamber as an electron beam with beam energy eV_B. The target plasma, which is the ion source plasma, is produced by this injected beam. This process constitutes single plasma operation. With the change of V_B and the beam current I_B, e_f in the target plasma (the source region of the ion source, which is the region of $H_2(v'')$ or $D_2(v'')$ production caused by e_f) are well controlled.[4,5] In the target plasma region, additional plasmas are produced with the discharge voltage V_t and current I_t, and are superimposed on the target plasmas, i.e., double plasma operation.

Plasma parameters (electron density n_e, electron temperature T_e, plasma space potential V_s and floating potential V_f) are measured using Langmuir probes. To obtain the electron energy distribution function (EEDF), the Druyvesteyn method was used. From the EEDF data, the density of fast electrons $n_{fe}(E)$ with an energy higher than E was estimated. The right end plate, the plasma grid, has a single hole (5 mm diameter) through which ions were extracted from the source. A magnetic-deflection-type ion analyzer and Faraday cup were used for relative measurement of the extracted H^- or D^- ions.

An electron beam is applied at z = 0 cm, which corresponds to the position of the mesh grid, and plasma is produced. Here, we refer to this plasma as an electron-beam-excited (EBE) plasma. There is a spatial variation in n_e (n_e increases gradually with z and then saturates near z = 15-17 cm), although T_e maintains a nearly constant value. Both n_e and T_e change markedly across the magnetic filter as that observed in the conventional tandem volume source, where filter position z_f = 20 cm.

Figure 2 shows the plasma parameters (n_e and T_e) in the first chamber (the source region) and in the second chamber (the extraction region), respectively, as a function of discharge power P_d. They are measured at z = 15 cm in the source region and at z = 21 cm in the extraction region, where the plasma grid is set at z = 22 cm. In the case of the single plasma, $P_d = V_B \cdot I_B$. Here, I_B is the current collected by the mesh grid. Since the geometric factor of the mesh grid for permeability is about 50 %, we assume that the injected beam current is equal to I_B. In the case of the double plasma, $P_d = V_B \cdot I_B + V_t \cdot I_t$, where V_t = 50 V and I_t = 2 A. When V_B is kept constant at a certain voltage (100 V in the single plasma and 80 V in the double plasma), I_B increases with increasing I_d, and then discharge power, $V_B \cdot I_B$, for the target plasma region increases. To obtain the data shown in Fig.2, in the single plasma operation, I_B is varied from 1 to 2.5 A. On the other hand, in the double plasma operation, I_B is varied from 0.63 to 2.5 A.

In the extraction region, due to the magnetic filter effect, electron temperature $T_e(2)$ maintains a nearly constant value which is lower than $T_e(1)$ in the source region, although n_e increases linearly with increasing I_d.

Figure 3 shows the dependence of the EEDF on P_d in the source region, corresponding to the results in Fig.2. These EEDF are also measured at z = 15 cm. With increasing P_d, the EEDF increases in magnitude, especially in the high-energy tail. The EEDF shows marked difference between single and double plasmas. This point is consistent with the differences in $n_e(1)$ and $T_e(1)$ shown in Fig.2. Namely, $n_e(1)$ and $T_e(1)$ in the single plasma are apparently lower than that in the double plasma. The aim of applying double plasma operation is to synthesize an optimum EEDF for negative ion formation. Ideally, one source is used for production of bulk plasma electrons and the other source for production of high-energy electrons. Although the present experiment does not always proceed ideally, double plasma operation is more effective for optimization of EEDF than single plasma operation.

Figure 4 shows the dependence of negative ion currents on P_d. Gas pressure p = 4 mTorr and extraction voltage V_{ex} = 400 V. Since the plasma grid is set at z = 22 cm in this case, the distance between the plasma grid and the magnetic filter is 2 cm. The plasma grid potential V_b is kept at earth potential, which is the potential of the chamber. Under the present operating conditions, however, the plasma grid is nearly optimal for extraction of the highest H^- current at every

I_d. The negative ion currents in the double plasma are nearly two times higher than those in the single plasma.

According to the dependence of $n_{Te}(1)$ on P_d, $n_{Te}(1)$ in the double plasma is higher than that in the single plasma. This tendency is consistent with that of the negative ion currents shown in Fig.4.

In Fig.4, the single plasma is operated only by EBE plasma. Therefore, it is important to know whether EBE plasma or filament discharge plasma (V_t-I_t discharge) is effective for H^- production. Figure 5 shows the dependence of H^- currents on P_d, where the plasma production method is a parameter. At the same P_d, H^- current has a tendency to increase slightly with I_t or I_B. Under the same discharge conditions, however, H^- currents are nearly equal to each other for the two plasma production methods. Comparing the H^- currents in Fig.5 with the H^- currents in Fig.4, it is reconfirmed that the H^- currents in the single plasma do not exceed the H^- currents in the double plasma.

As is discussed elsewhere,[4,5] when H^- ions are produced using the so-called two-step process where $H_2(v'')$ are produced in the source region and H^- ions are formed in the extraction region, H^- density is written as

$$H^- \text{ density} = n_{Te}(1)\, n_e(2)\, N_{H2} \langle \sigma v \rangle_{v''} \langle \sigma v \rangle_{DA}\ \tau_{v''}\ \tau_-,$$

where $n_{Te}(1)$ is e_T density in the source region, $n_e(2)$ is n_e in the extraction region, N_{H2} is density of hydrogen molecules, $\langle \sigma v \rangle_{v''}$ is reaction rate of vibrational excitation by e_T in the source region, $\langle \sigma v \rangle_{DA}$ is reaction rate of dissociative attachment in the extraction region, $\tau_{v''}$ is the lifetime of $H_2(v'')$, and τ_- is the lifetime of H^- ions. Although these reaction rates and lifetimes depend on T_e, roughly speaking, H^- density is proportional to the product of $n_{Te}(1)$ and $n_e(2)$,[4,5] if T_e maintains a certain constant value during the change of electron densities. The production process of D^- ions is believed to be the same as that of H^- ions.

Enhancement of H^- production in the double plasma operation is well explained. According to the plasma parameters presented here, key parameters to the two-step negative ion production process, $n_{Te}(1)$, $T_e(1)$, $n_e(2)$ and $T_e(2)$, are optimized better in the double plasma operation than in the single plasma operation.

D^- currents for D_2 discharge are also plotted, for reference, in Fig.4. Intensities of D^- currents are nearly the same as those of H^- currents. This suggests that the D^- density in the source is higher than the H^- density,[6] because extraction voltages are the same for both cases. So far, the isotope effects have been reported by several authors.[7-10] In general, the experimental results show that the negative ion current or density in D_2 plasmas is lower than that in H_2 plasmas. Recently, however, we have found that under the same operating conditions, the D^- current is higher than the H^- current, although discharge current is rather low.[6] In the present experiment, it is also confirmed that D^- current is higher than or equal to H^- current. This result differs from those of other experiments[7-10] and requires further investigation. Details on isotope effects will be discussed in the forthcoming paper.

In summary, we have studied the enhancement of H^- production achieved by controlling EEDF. Measurements of the basic plasma parameters have been performed in the source and extraction regions of the EBE plasma (single plasma) and the double plasma operating in H_2. For the same discharge power, H^- production in the double plasma operation is higher than that in the single plasma operation. It is also found that D^- current is nearly the same as H^- current under the same discharge conditions, although discharge power is rather low.

This work is supported in part by the Grant-in-Aid for Scientific Research from the Ministry of Education, Science and Culture.

References

1) O. Fukumasa: J. Phys. D: Appl. Phys. **22**(1989)1668.

2) O. Fukumasa: J. Appl. Phys. **71**(1992)3193.

3) J. R. Hiskes and A. M. Karo: J. Appl. Phys. **56**(1984)1927.

4) O. Fukumasa and T. Iwasaki: *Proc. 6th Inter. Symp. on the Production and Neutralization of Negative Ions and Beams*(AIP press, NW, 1994) p.411.

5) O. Fukumasa, T. Iwasaki, H. Naitou and S. Sakiyama: Rev. Sci. Instrum. **65**(1994)1210.

6) O. Fukumasa, H. Nishimura, S. Sakiyama and T. Kimoto: Rev. Sci. Instrum. **67**(1996)1396.

7) T. Inoue, G. D. Ackerman, W. S. Cooper, M. Hanada, J. W. Kwan, Y. Ohara, Y. Okumura and M. Seki: Rev. Sci. Instrum. **61**(1990)496.

8) R. Leroy, M. Bacal, P. Berlemont, C. Courteille and R. A. Stern: Rev. Sci. Instrum. **63**(1992)2686.

9) D. A. Skinner, A. M. Bruneteau, P. Berlemont, C. Courteille, R. Leroy and M. Bacal: Phys. Rev. **E 48**(1993)2122.

10) W. G. Graham: *Proc. 6th Inter. Symp. on the Production and Neutralization of Negative Ions and Beams*(AIP press, NW, 1994) p.90.

Figure Captions

Fig. 1. Schematic diagram of the double plasma negative ion source.

Fig. 2. Plasma parameters (n_e and T_e) in the source region and in the extraction region versus discharge power P_d, where $P_d = V_B \cdot I_B$ in the single plasma operation and $P_d = V_B \cdot I_B + V_t \cdot I_t$ in the double plasma operation. Parameters in the source region (filled symbols) and those in the extraction region (open symbols) are measured at z = 15 and 21 cm, respectively. The electron beam is injected into the target plasma at z = 0, and the magnetic filter and the plasma grid are set at z = 20 and 22 cm, respectively. Experimental conditions are as follows: V_d = 40 V, p(H_2 gas) = 4 mTorr and V_B = 80 V in the double plasma operation and 100 V in the single plasma operation.

Fig. 3. Electron energy distribution functions (EEDF) for H_2 plasmas in the source region versus P_d, (a) bulk plasma electrons and (b) high-energy tail. EEDF are measured at z = 15 cm. The experimental conditions are the same as those in Fig.2.

Fig. 4. Extracted H^- currents versus P_d, where plasma grid potential V_b is set to be equal to that of the anode. The experimental conditions are the same as those in Fig.2 except that extraction voltage V_{ex} = 400 V.

Fig.5. Extracted H^- currents versus P_d, where parameters are V_B and V_t. For the EBE plasma (filled symbols), I_B is varied from 1 to 2 A for three different V_B, 40 (triangles), 60 (squares) and 80 (circles) V. In the case of filament discharge (open symbols), I_t is varied from 1 to 2 A for three different V_t, 40 (triangles), 60(squares) and 80(circles) V.

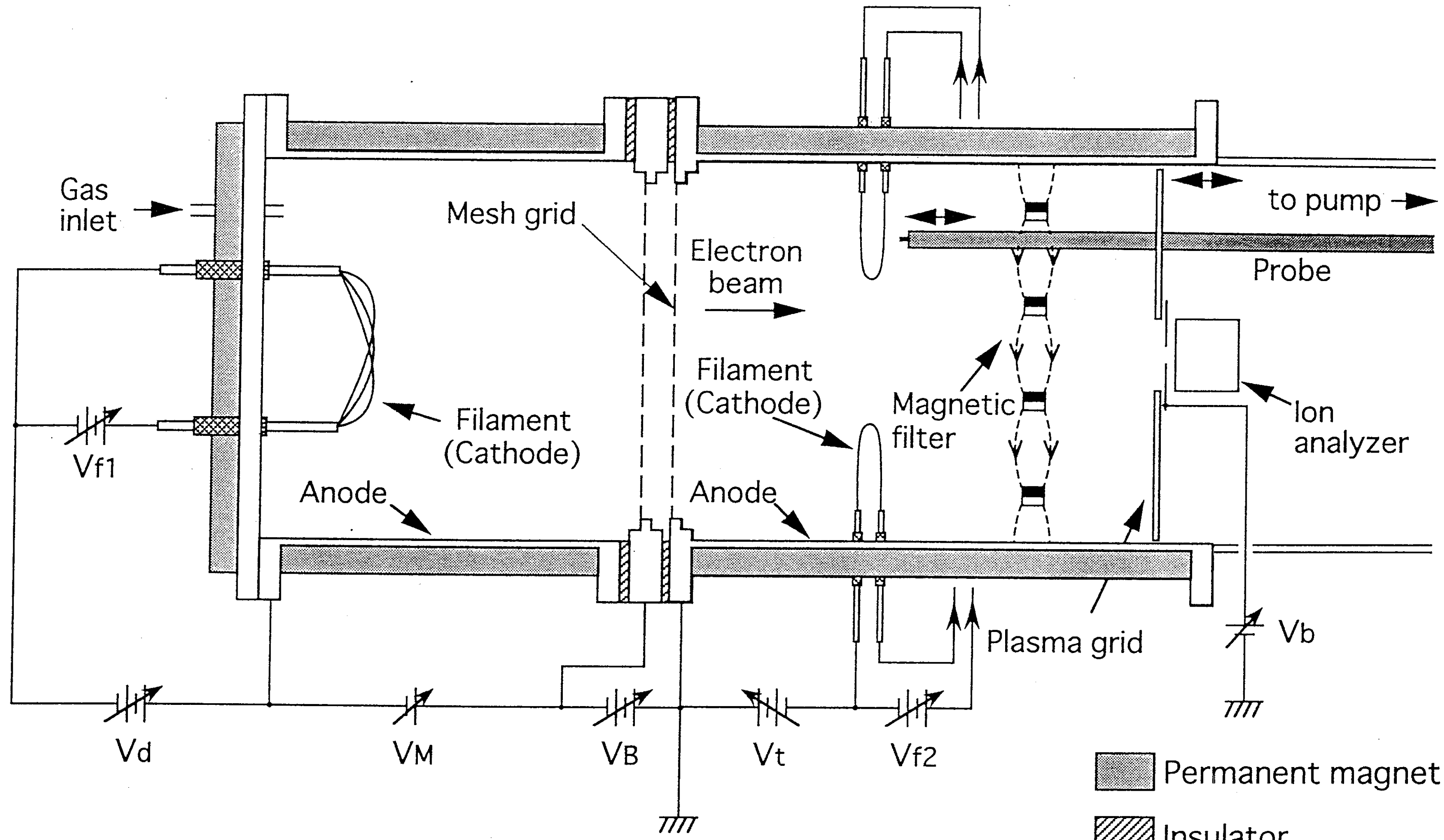

Fig. 1 O. Fukumasa (10)

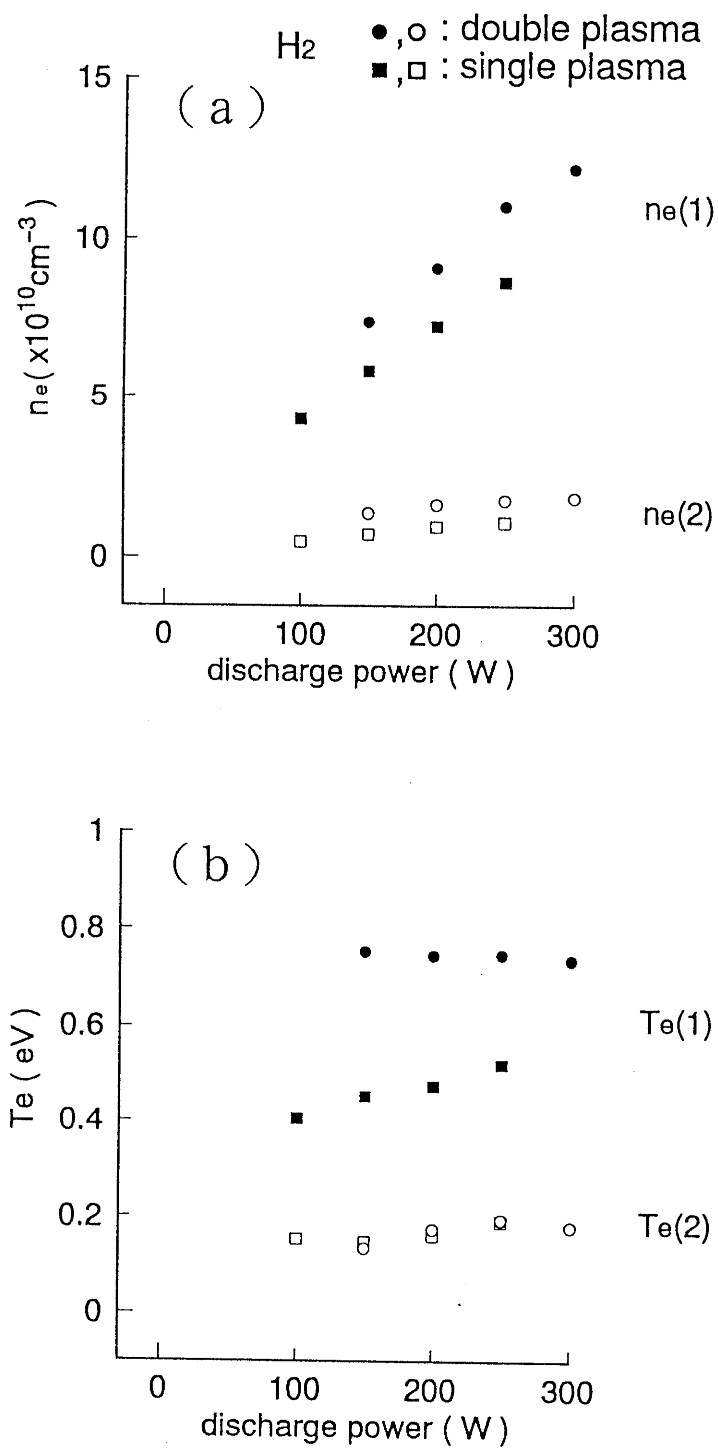

Fig. 2 O. Fukumasa ⑧

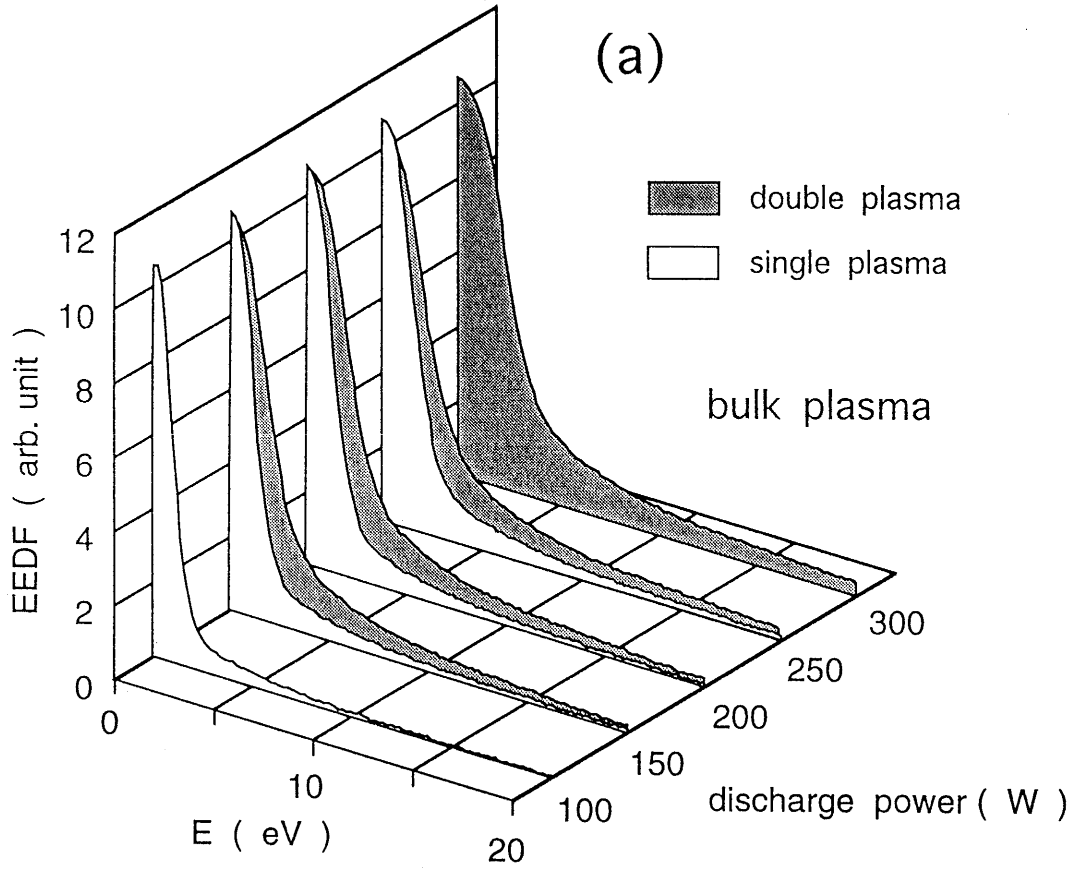

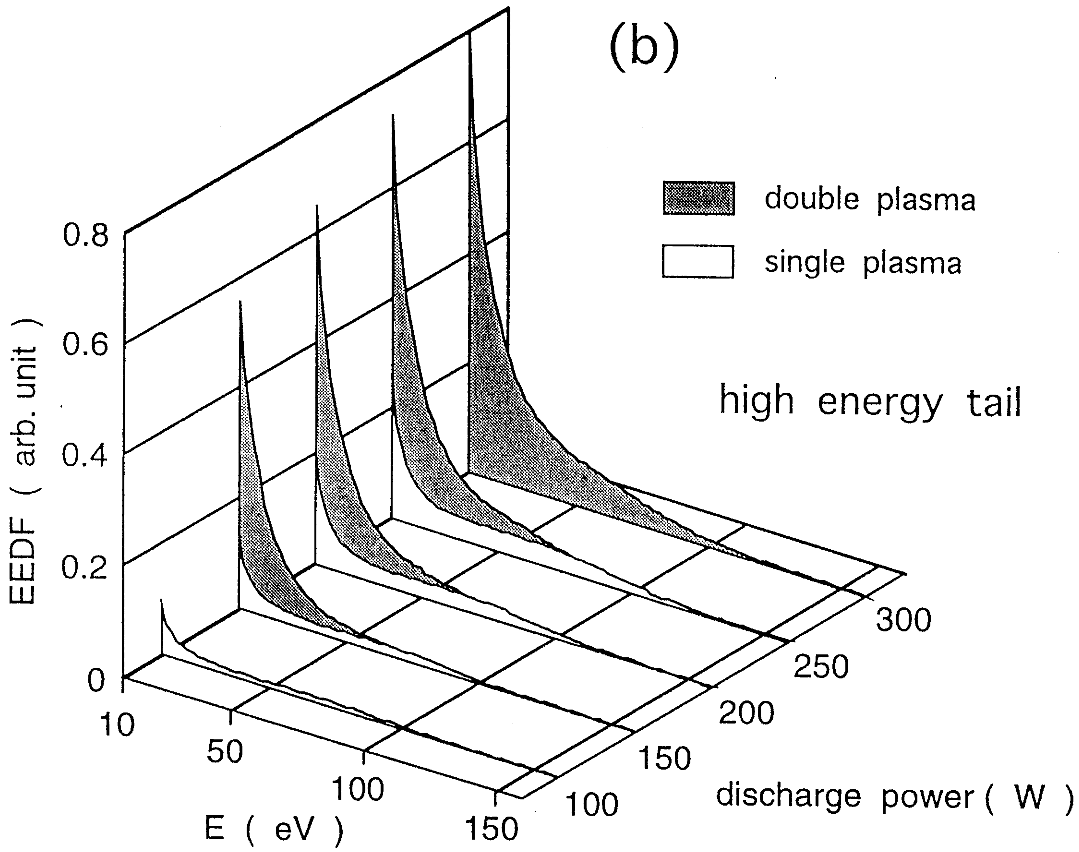

Fig. 3 O. Fukumasa (8)

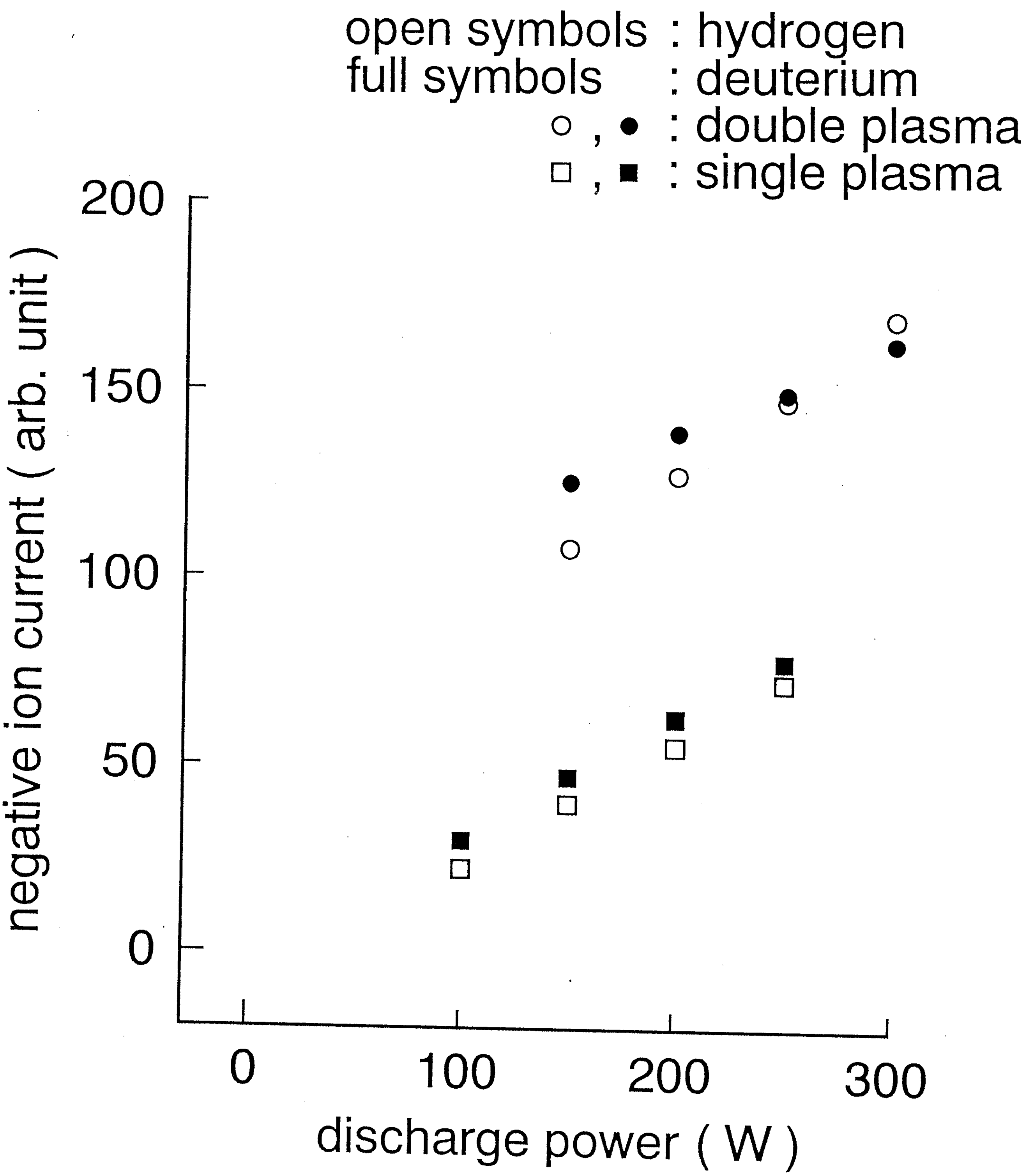

Fig. 4 O. Fukumasa (8)

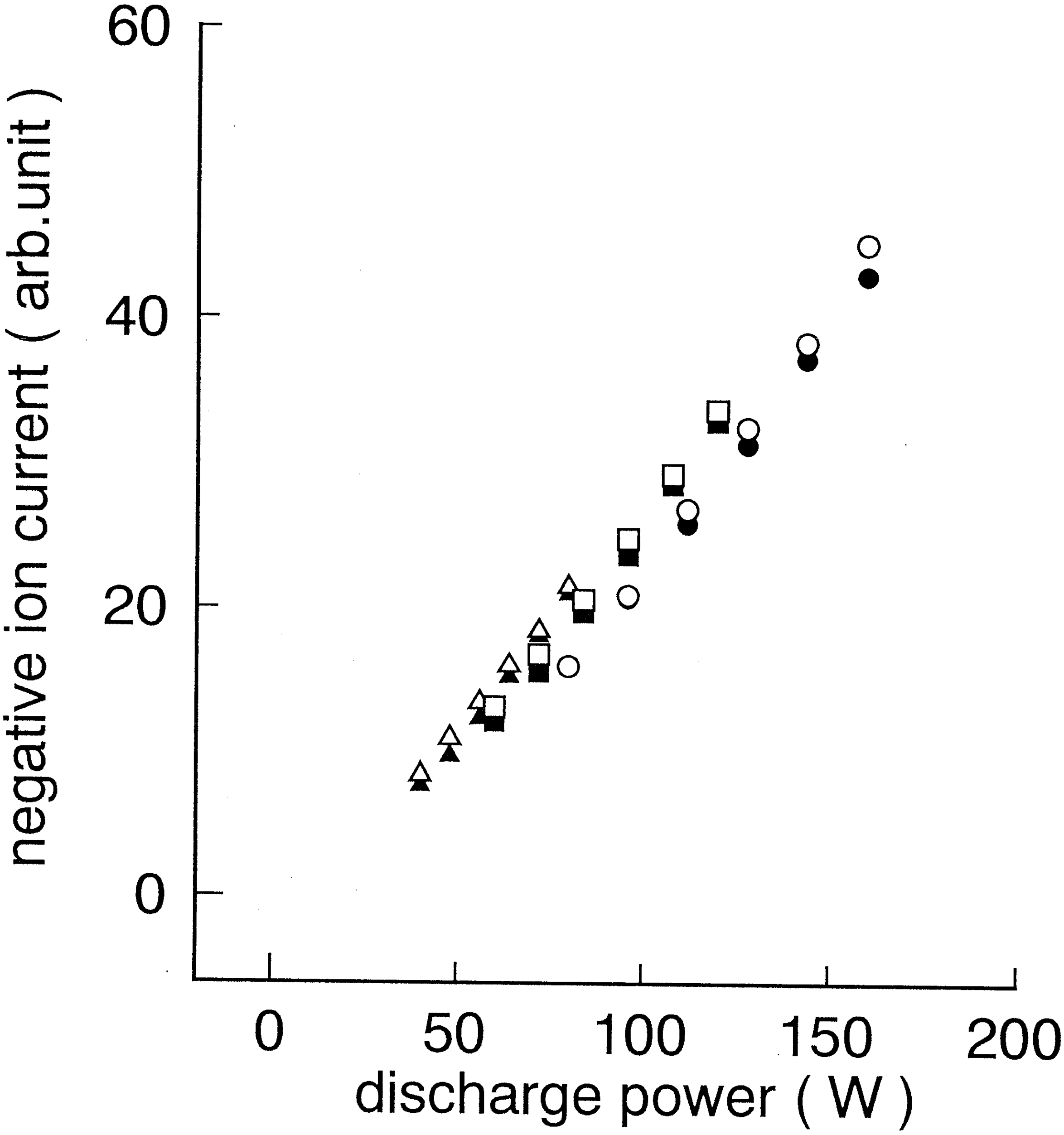

Fig. 5 O. Fukumasa ⑧